NASA/TM—2010-216064 GT2009–60322

Three-Dimensional Unsteady Simulation of a Modern High Pressure Turbine Stage Using Phase Lag Periodicity: Analysis of Flow and Heat Transfer

Vikram Shyam
Glenn Research Center, Cleveland, Ohio

Ali Ameri, Daniel F. Luk, and Jen-Ping Chen
The Ohio State University, Columbus, Ohio

February 2010

NASA STI Program . . . in Profile

Since its founding, NASA has been dedicated to the advancement of aeronautics and space science. The NASA Scientific and Technical Information (STI) program plays a key part in helping NASA maintain this important role.

The NASA STI Program operates under the auspices of the Agency Chief Information Officer. It collects, organizes, provides for archiving, and disseminates NASA's STI. The NASA STI program provides access to the NASA Aeronautics and Space Database and its public interface, the NASA Technical Reports Server, thus providing one of the largest collections of aeronautical and space science STI in the world. Results are published in both non-NASA channels and by NASA in the NASA STI Report Series, which includes the following report types:

- TECHNICAL PUBLICATION. Reports of completed research or a major significant phase of research that present the results of NASA programs and include extensive data or theoretical analysis. Includes compilations of significant scientific and technical data and information deemed to be of continuing reference value. NASA counterpart of peer-reviewed formal professional papers but has less stringent limitations on manuscript length and extent of graphic presentations.

- TECHNICAL MEMORANDUM. Scientific and technical findings that are preliminary or of specialized interest, e.g., quick release reports, working papers, and bibliographies that contain minimal annotation. Does not contain extensive analysis.

- CONTRACTOR REPORT. Scientific and technical findings by NASA-sponsored contractors and grantees.

- CONFERENCE PUBLICATION. Collected papers from scientific and technical conferences, symposia, seminars, or other meetings sponsored or cosponsored by NASA.

- SPECIAL PUBLICATION. Scientific, technical, or historical information from NASA programs, projects, and missions, often concerned with subjects having substantial public interest.

- TECHNICAL TRANSLATION. English-language translations of foreign scientific and technical material pertinent to NASA's mission.

Specialized services also include creating custom thesauri, building customized databases, organizing and publishing research results.

For more information about the NASA STI program, see the following:

- Access the NASA STI program home page at *http://www.sti.nasa.gov*

- E-mail your question via the Internet to *help@sti.nasa.gov*

- Fax your question to the NASA STI Help Desk at 443–757–5803

- Telephone the NASA STI Help Desk at 443–757–5802

- Write to:
  NASA Center for AeroSpace Information (CASI)
  7115 Standard Drive
  Hanover, MD 21076–1320

NASA/TM—2010-216064 GT2009–60322

Three-Dimensional Unsteady Simulation of a Modern High Pressure Turbine Stage Using Phase Lag Periodicity: Analysis of Flow and Heat Transfer

Vikram Shyam
Glenn Research Center, Cleveland, Ohio

Ali Ameri, Daniel F. Luk, and Jen-Ping Chen
The Ohio State University, Columbus, Ohio

Prepared for the
Turbo Expo 2009
sponsored by the American Society of Mechanical Engineers
Orlando, Florida, June 8–12, 2009

National Aeronautics and
Space Administration

Glenn Research Center
Cleveland, Ohio 44135

February 2010

Acknowledgments

We are grateful to Dr. James Heidmann of NASA Glenn Research Center, Dr. Meyer Benzakein of The Ohio State University and to AVETEC for funding various segments of this research effort. We would like to acknowledge Dr. Wai-Ming To of The University of Toledo for his numerous useful insights and discussions, The Ohio Super Computing Center for computing resources and NASA Glenn Research Center, where the first author is a co-op and the second author is a resident researcher.

This work was sponsored by the Fundamental Aeronautics Program at the NASA Glenn Research Center.

Level of Review: This material has been technically reviewed by technical management.

Available from

NASA Center for Aerospace Information
7115 Standard Drive
Hanover, MD 21076–1320

National Technical Information Service
5285 Port Royal Road
Springfield, VA 22161

Available electronically at http://gltrs.grc.nasa.gov

Three-Dimensional Unsteady Simulation of a Modern High Pressure Turbine Stage Using Phase Lag Periodicity: Analysis of Flow and Heat Transfer

Vikram Shyam
National Aeronautics and Space Administration
Glenn Research Center
Cleveland, Ohio 44135

Ali Ameri, Daniel F. Luk, and Jen-Ping Chen
The Ohio State University
Columbus, Ohio 43210

Abstract

Unsteady three-dimensional RANS simulations have been performed on a highly loaded transonic turbine stage and results are compared to steady calculations as well as experiment. A low Reynolds number k-ε turbulence model is employed to provide closure for the RANS system. A phase-lag boundary condition is used in the periodic direction. This allows the unsteady simulation to be performed by using only one blade from each of the two rows. The objective of this paper is to study the effect of unsteadiness on rotor heat transfer and to glean any insight into unsteady flow physics. The role of the stator wake passing on the pressure distribution at the leading edge is also studied. The simulated heat transfer and pressure results agreed favorably with experiment. The time-averaged heat transfer predicted by the unsteady simulation is higher than the heat transfer predicted by the steady simulation everywhere except at the leading edge. The shock structure formed due to stator-rotor interaction was analyzed. Heat transfer and pressure at the hub and casing were also studied. Thermal segregation was observed that leads to the heat transfer patterns predicted by steady and unsteady simulations to be different.

Nomenclature

μ	Coefficient of viscosity
ρ	Density
CFD	Computational Fluid Dynamics
T	Temperature
St	Stanton Number
n	normal distance from surface
P	Static pressure normalized by Reference pressure
Pr	Prandtl Number
Re	Reynolds Number
S	Normalized distance along blade surface at a given span, with $S = 0$ at leading edge
V	Magnitude of velocity
$\|Z\|$	Absolute value of z-coordinate in blade to blade direction
R	Radius measured from axis of rotation
Δ	Percent difference

Subscripts

ref	Reference conditions
wall	solid surface (no slip boundary)
inlet	Inlet to the rotor
steady	Refers to solution variables resulting from a steady simulation
time-averaged	Refers to solution variables obtained by time-averaging the results of an unsteady simulation

Introduction

It is well known that flow through the high pressure turbine is highly unsteady primarily due to the interactions of the passing wake and, in the case of transonic stages, shock structures. This unsteadiness is particularly important to film cooling applications at the rotor leading edge. It is possible that the pressure at the leading edge may rise to such an extent that the leading edge cooling holes suck hot air in rather than blow cool air out. It is therefore important to understand the nature of unsteadiness with regard to both pressure and heat transfer at the leading edge as well as the rotor tip.

Hodson and Dawes (Ref. 1) studied the effect of unsteadiness on exit profiles emerging from a two-dimensional multiblade row cascade subject to unsteady wakes at the inlet. They detailed the distortion of the wake through chopping, stretching and shearing by the neighboring blade row. The vortex structure between blades downstream of the unsteady wake, they suggest, tends to push the flow from the pressure side to the suction side. This pushes the stagnation point closer to the crown of the blade rather than the leading edge. Denos et al. (Ref. 2) also observed this effect and noted that the stator trailing edge shock moves from the

crown of the rotor towards the leading edge with the passage of the wake from the upstream stator. For their study, Denos et al. (Ref. 2) used the implicit time marching code MDFLOS3D that solves the unsteady Favre-averaged Navier-Stokes equations in a quasi-three-dimensional manner. Only the rotor mid-span was analyzed.

Shang and Epstein (Ref. 3) found that a nonuniform inlet profile resulting from an unsteady wake would lead to a segregation effect that would push hot gas preferentially towards one side of the blade. Ameri et al. (Ref. 4) also noted the effect that segregation might have on blade heat transfer. This segregation as described by Kerrebrock and Mikolajczak (Ref. 5) occurs because the Mach number profile in the circumferential direction stays approximately constant while the rotor wake, having a lower temperature, forces the local absolute velocity to diminish thus producing a relative velocity which is at a shallower angle to the axial. Thus, the cooler wake flow and hotter free stream flow would be distributed at different angles. The phenomenon would be absent in the case of a steady simulation and it would be expected that a steady and an unsteady computation lead to different heat transfer patterns on the blade surface.

Bell and He (Ref. 6) performed an experiment to study the tip leakage on an oscillating blade. They found that the unsteadiness in the tip gap flow field is primarily an inviscid effect by comparing their data to an inviscid simulation.

Urbassik et al. (Ref. 7) conducted experimental investigations on vane-rotor aerodynamic interactions and found that while unsteadiness is caused by a combination of shocks, potential fields and vane wake interactions, the upstream wake has little influence on rotor unsteadiness.

Ameri et al. (Ref. 4) performed an unsteady, three-dimensional simulation on the E^3 turbine blade geometry. They used a sinusoidal inlet profile to simulate an unsteady wake and assumed a 1:1 stator to rotor blade count. They found significant differences between the unsteady and steady heat transfer results in localized regions, particularly in the near tip and near hub regions on the suction side of the blade. Although a general rise in the level of heat transfer was predicted by the unsteady simulations compared to the steady simulations they found no substantial difference in the tip heat transfer. Tip heat transfer is however highly dependent on airfoil geometry.

For the case being considered here, Tallman et al. (Ref. 8) and Luk (Ref. 9) obtained steady state heat transfer and pressure results from CFD simulations using TACOMA (Ref. 10) and TURBO (Refs. 11 to 13), respectively. The former used a k-ω turbulence model while the latter used the k-ε model of Zhu and Shih (Ref. 14) that is also used in this paper. The surface pressure and heat transfer results matched well with experiment for both cases (Tallman only shows mid-span comparisons). Both authors observed the presence of a shock between the trailing edge of a rotor blade and the suction surface of the adjacent rotor blade.

Van Zante et al. (Ref. 15) performed simulations on a 2 1/2 stage compressor and found that phase lagged boundary conditions are only accurate for single-stage cases and do not account for stator-stator or rotor-rotor interaction for multistage cases. The current study involves a stator-rotor interaction within a single stage and is therefore able to employ the phase lag condition to accurately represent unsteadiness. It was also found that owing to the storage of time history for the phase lag model, convergence requires more time than for the periodic model for multistage cases. However the advantage of using phase lag is that only one blade passage from each row is required for the simulation. Gerolymos et al. (Ref. 16) also used phase lag (chorocronicity) to verify the ability of this boundary condition to predict shock interactions between two neighboring blade rows. They also provide a list of studies conducted by various authors on blade-row interaction.

Previous computational studies have dealt with two-dimensional cascades (Refs. 1 and 17) or have assumed a periodic inlet boundary (Ref. 4) to the rotor to simulate unsteadiness. In general, unsteadiness has been computed by compromising either the dimensionality of the flow or frequency of unsteadiness. This paper is believed to be the first unsteady three-dimensional CFD simulation of heat transfer on a highly loaded transonic turbine stage. This is accomplished using a phase lagged boundary condition in the pitch-wise direction. The implementation and theory behind this boundary condition can be found in several publications such as References 12, 13, and 16. This paper will also serve as a validation for both the turbulence model and phase lag boundary condition for unsteady heat transfer prediction.

Numerical Simulation

The simulation was performed using the unsteady, viscous, three-dimensional RANS code TURBO. A modified high order, upwind Roe scheme is employed for spatial discretization with Newton sub-iterations to converge the solution at every time step. Due to the upwinding scheme used in this simulation there is no addition of artificial dissipation. The simulation is third order accurate in space and second order accurate in time. The low Reynolds number k-ε turbulence model of Shih (Ref. 14) is used. This model integrates to the wall without the use of wall functions. The code is fully parallelized to use MPI (Message Passing Interface) (Refs. 13 and 18).

A highly loaded high pressure turbine stage (Ref. 8) was used for this study and consists of 38 stators and 72 rotors that rotate at approximately 9000 rpm. The rotor blade is highly three-dimensional with a tip clearance of 2.1 percent of the blade span. An O-H grid (O grid around the blade and H grid for the rest of the domain) was generated using GridPro (Program Development Company) and results in a $y+<<1$. The domain was partitioned into 20 blocks for

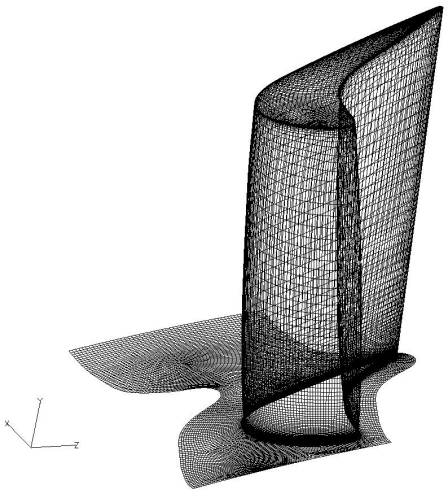

Figure 1.—Rotor grid.

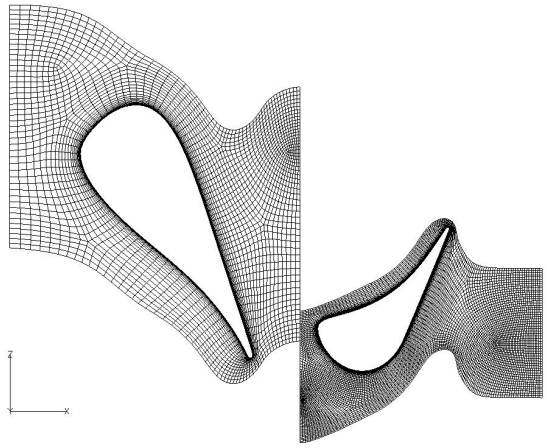

Figure 2.—Relative stator-rotor positioning for unsteady case.

the rotor and 11 blocks for the stator. The grid consists of 2,461,740 cells of which 1,751,840 cells represent the rotor grid. In the radial direction 156 cells are used while 101 cells fill the rotor-to-rotor (circumferential) region. Figure 1 shows the grid on the rotor. Figure 2 shows the relative positions and sizes of the vane and rotor grids. Previous studies such as the one by Green et al. (Ref. 19) using grid sizes smaller than the current grid have shown satisfactory results, hence this grid is considered fine enough that no grid-refinement study was deemed necessary.

The unsteady simulation was run for approximately 11 complete revolutions of the rotor blade row. Convergence was monitored by observing mass-flow values at stator inlet and rotor exit as well as surface heat transfer on the rotor blade over several iterations. For the steady case, the solution was deemed converged when surface pressure and heat transfer, 1000 iterations apart, were nearly indistinguishable. In both cases the solution was initialized ab initio.

An in-house developed preprocessor was used to setup the case by converting GridPro connectivity and boundary information to a format compatible for use with TURBO. The Reynolds number of the flow was approximately 3×10^6 per unit length and is consistent with Tallman et al. (Ref. 8). An isothermal boundary condition was used for all solid surfaces and the wall temperature was set to 0.7 times the reference temperature to simulate realistic flow conditions. The isothermal boundary condition, added for the purpose of heat transfer simulation, has been validated for an unpublished flat plate case. Post processing and visualization in this study were realized through TecPlot (TecPlot Inc.) and Fieldview (Intelligent Light).

Steady Case

For the steady case, the vane was first simulated and the exit total pressure and temperature profiles obtained from the vane were circumferentially averaged and used for the inlet of the rotor. The profiles were thus radial in nature. Periodic boundaries were specified at the circumferential extremities. Results from this case can be found in Luk (Ref. 9).

Unsteady Case

An inlet profile of total temperature and total pressure upstream of the vane were specified based on the experimental data of Tallman et al. (Ref. 8). Radial static pressure distribution downstream of the blade was specified. This pressure distribution itself was a product of an unsteady computation for a 1 1/2 stage simulation performed by Green (Ref. 19). Phase lag boundary condition was used in the circumferential direction to account for unsteadiness and 50 time steps per blade passage were computed. Phase lag assumes that a blade row is periodic with the frequency of wake passage of the neighboring blade row (Ref. 12). This requires that solution history be stored for one period of wake passing. At the stator-rotor interface, a sliding interface boundary condition was imposed. The code TURBO, in its present form, requires the grid lines at the stator exit and rotor inlet to match radially but does not require them to match in the circumferential direction. The simulation took approximately 150,000 iterations to converge.

Figure 3 shows a comparison between the rotor inlet profiles for (i) total pressure and (ii) total temperature at (a) 15 percent span, (b) 50 percent span and (c) 90 percent span. The abscissa in Figure 3 represents the blade to blade or circumferential direction across one rotor blade passage. The black line represents the steady simulation while the red line shows the time-average of the unsteady simulation. It is clear from the figures that the time averaged total pressure profiles, are fairly well predicted by the steady profiles. However, the total temperature profiles for the steady case are higher than the

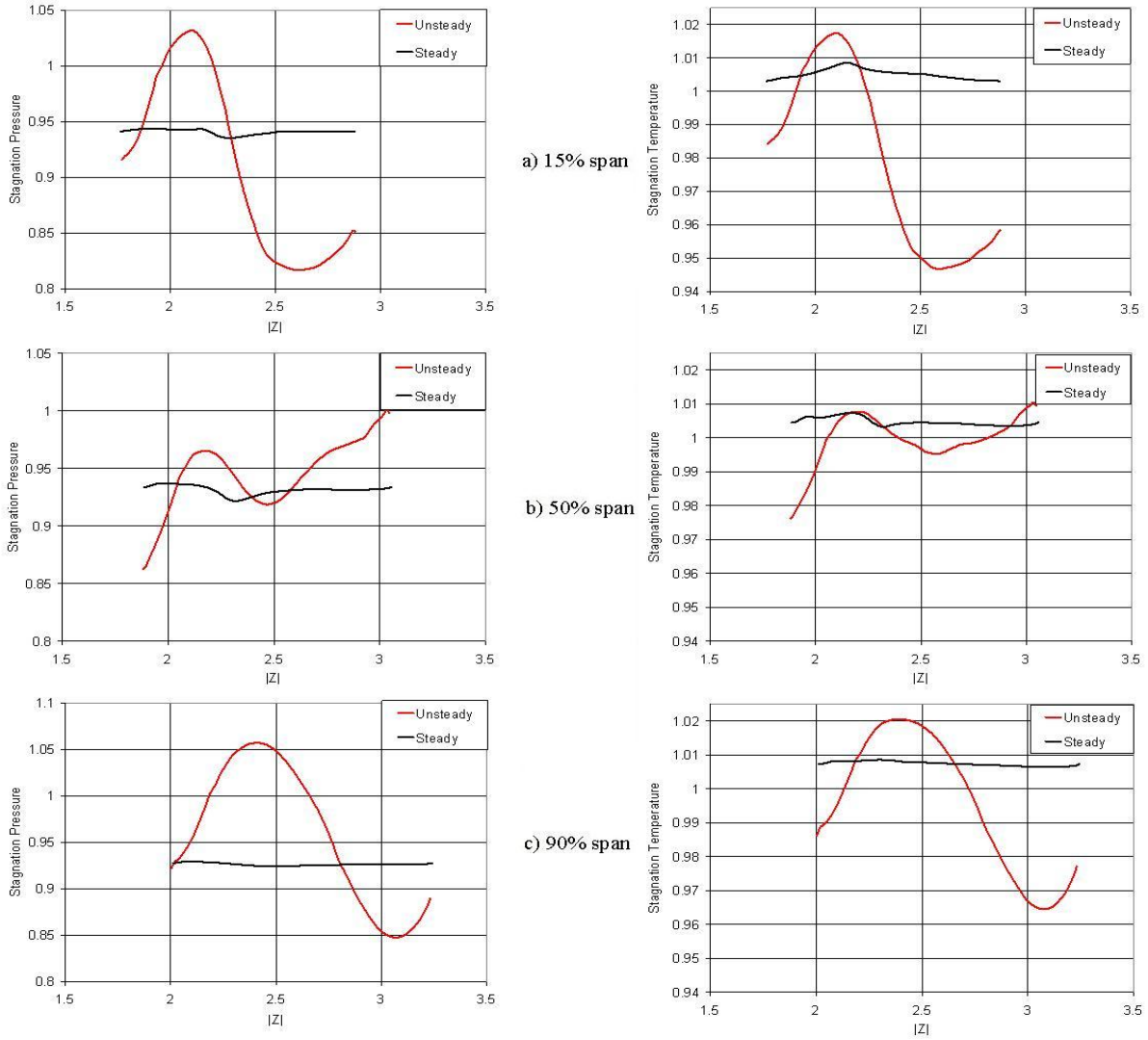

Figure 3.—Comparison of steady and time-averaged rotor inlet profiles of total pressure and total temperature.

time-average of the unsteady total temperature. This could have a significant impact on the heat transfer predictions as will be shown in subsequent sections. Both the pressure and temperature profiles are plotted for one passage of the rotor blade and are not therefore a complete period.

Rotor Blade Analysis

Steady and Time-Averaged Results

The following sections will show pressure ratio, P, and heat transfer results in the form of Stanton number, St, computed as,

$$St = -\left[\frac{\left.\frac{dT}{dn}\right|_{\text{wall}}}{T_{\text{wall}} - T_{\text{ref}}}\right] \cdot \left[\frac{\mu_{\text{wall}}}{(\rho V)_{\text{inlet}}}\right] \cdot \frac{1}{\text{Re}_{\text{ref}} \cdot \text{Pr}} \qquad (1)$$

In the figures to follow, the abscissa is the normalized distance, S, along the blade surface with –1 to 0 representing the pressure surface from trailing edge to leading edge and 0 to 1 representing the suction surface from leading edge to trailing edge. The Stanton number as presented is in reality a normalized wall heat flux. It is normalized by T_{wall} and T_{ref} which are both constants. Figure 4(i) shows the pressure distribution along the blade surface at (a) 15 percent span, (b) 50 percent span and (c) 90 percent span.

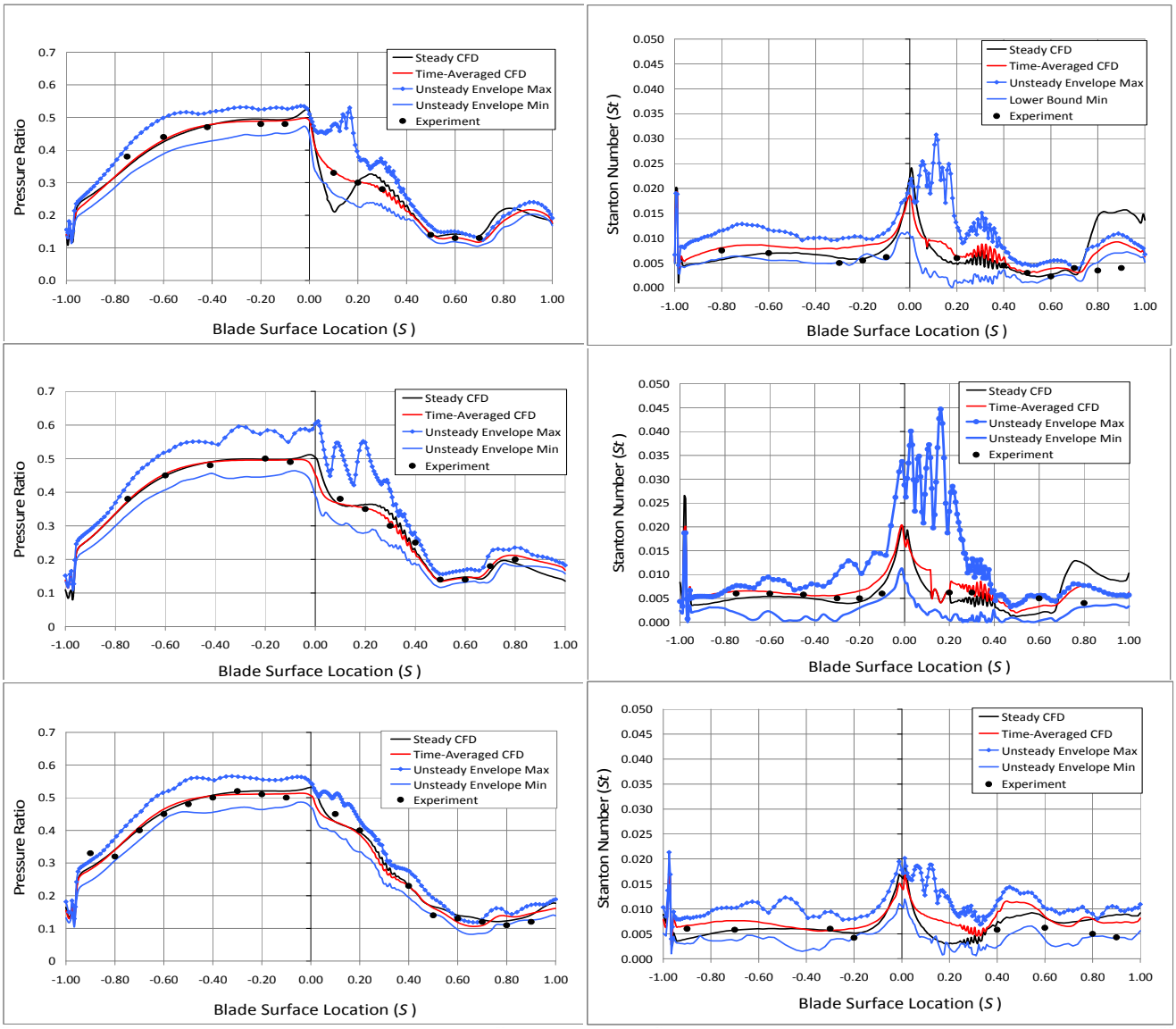

Figure 4.—Comparison of steady and time-averaged unsteady pressure and Stanton number to experiment at various span locations along the rotor blade.

The unsteadiness at the hub and case cause the steady solution to deviate from the data in the vicinity of the leading edge, $S = 0$. Overall, the time averaged pressure results match with the data better than the steady solution. Figure 4(ii) shows Stanton number along the rotor blade surface at (a) 15 percent span, (b) 50 percent span and (c) 90 percent span. Figure 3 shows that the inlet total temperature for the unsteady case is lower than the inlet total temperature for the steady case causing the Stanton number at the leading edge to be higher for the steady case than for the time-average of the unsteady case. The Stanton number is normalized by the difference between wall temperature and reference temperature. In the future Stanton number could be normalized using adiabatic wall temperature instead of inlet total temperature as recommended by Ameri et al. (Ref. 4). This would eliminate any dependence of the heat transfer coefficient on the inlet temperature profile.

It appears from Figure 4(ii) that at the 90 percent span the effect of unsteadiness is at its minimum. The oscillations between $S = 0.2$ to 0.4 are possibly due to the upwinding method. This is the location of the interaction of the shock and wake emanating from the upstream vane. There is a sharp rise in Stanton number and pressure starting at $S = 0.7$. This is consistent with the rotor trailing edge shock. It appears that the shock also triggers transition from laminar to turbulent flow although this is less evident near the tip. This indicates that the flow over the blade is largely laminar, contrary to what is reported in Tallman et al. (Ref. 8). This abrupt rise is not visible at the 90 percent span location due to the leakage at the tip.

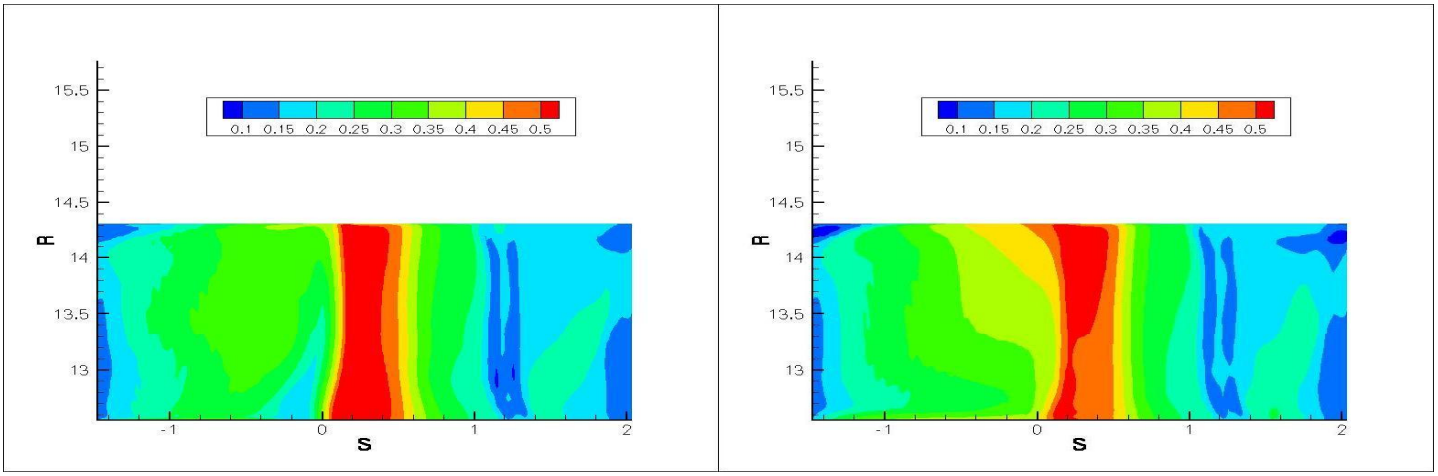

(a) Steady (b) Time-averaged

Figure 5.—Pressure distribution on unfolded rotor blade surface.

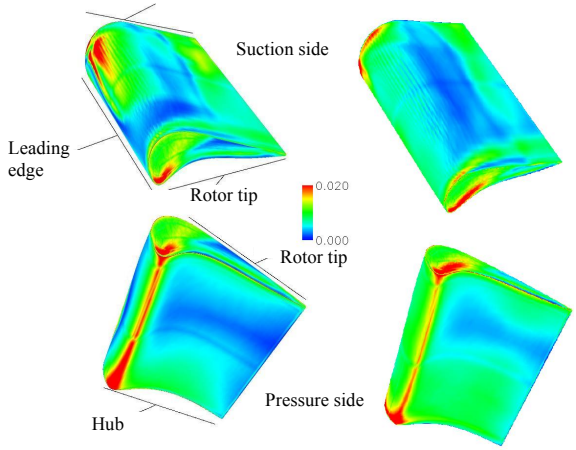

(a) Steady (b) Time-averaged

Figure 6.—Comparison between steady (Ref. 8) and time-averaged Stanton number distribution on rotor blade suction side (top) and pressure side (bottom).

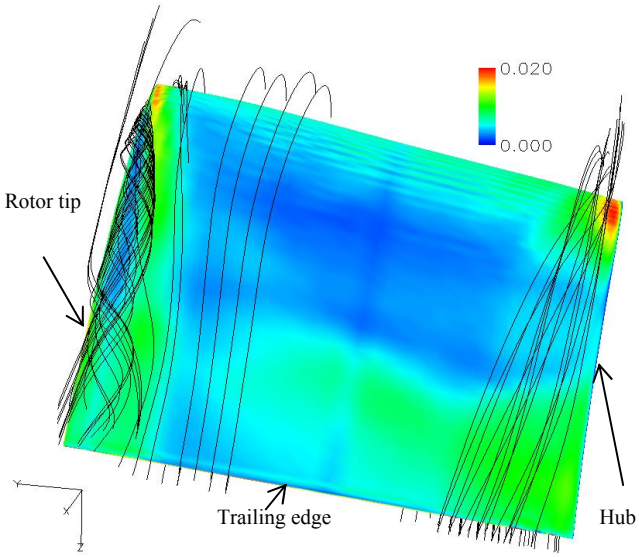

Figure 7.—Streamlines of relative velocity over suction side of rotor blade with rotor blade showing Stanton number contours.

Figure 5(a) shows the steady pressure distribution on the entire unfolded rotor blade. Figure 5(b) shows the time-average of unsteady pressure. It is clear that the effect of unsteadiness is observed mainly along the leading edge. Here, *R*, is the radial location and increases from hub to rotor tip.

Figure 6(a) shows the distribution of Stanton number on the rotor from the steady simulation and Figure 6(b) shows the time-averaged Stanton number. The suction side is shown at the top and the pressure side at the bottom of Figure 6. Unlike in the case of pressure, the overall Stanton number levels are higher for the time-averaged case over most of the rotor blade surface. This observation is consistent with that of Ameri et al. (Ref. 4). However, at the leading edge the steady case predicts higher heat transfer than the unsteady case and this may be explained by examining Figure 3 as explained in a previous section. Some islands of higher temperature and pressure are observed near the suction side trailing edge and could be due to tip-leakage. Figure 8 also shows higher levels of heat transfer on the suction side, near the rotor tip. This is shown as a green streak starting near the rotor suction side leading edge and extending towards the trailing edge and radially towards the hub. This is caused by the scrubbing action of the tip leakage vortex as well as due to the high temperature gas within it which is sucked onto the suction side and causes higher heat transfer. This is easier to see in Figure 7 that shows streamlines over the suction side of the blade. The tip vortex can be seen and so can the streamlines near the hub that move radially toward the casing.

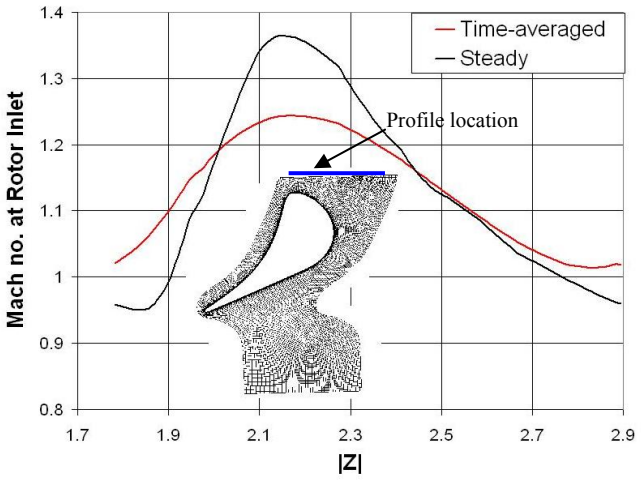

Figure 8.—Circumferential Mach number profile at 15 percent span at inlet to rotor.

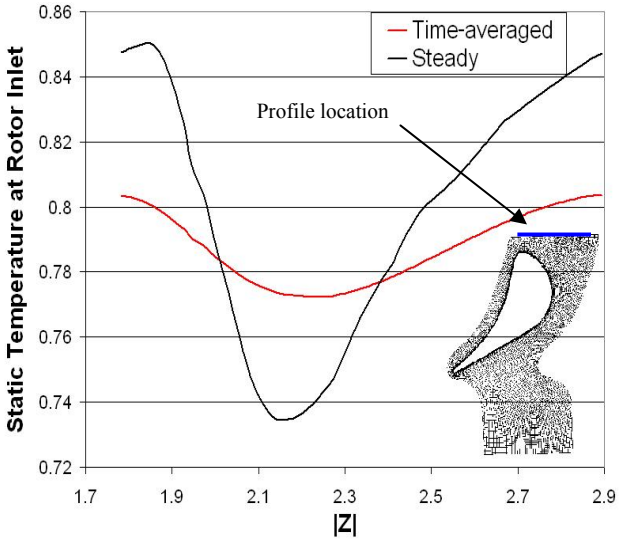

Figure 9.—Circumferential Static Temperature profile at 15 percent span at inlet to rotor.

The pattern of heat transfer distribution on the rotor blade is different for the steady case and for the time-averaged unsteady case. This is especially visible near the hub on the suction side, and near the hub and leading edge on the pressure side. This could be caused due to thermal segregation (Refs. 3 and 4).

As verification of this, Figures 8 and 9 show the Mach number and static temperature profiles in the circumferential direction at rotor inlet. An inlay of the rotor blade is included to aid in understanding the location of the profile. While the Mach number from the steady case and the unsteady case match fairly closely, the temperature profiles are very different. This leads to thermal segregation and a heat transfer pattern for the unsteady case that is different from the steady case.

The pressure distribution appears to be radial for a large portion of the blade except near the tip and the hub where it is highly three-dimensional due to the interaction of the passage flow with secondary flows from the hub and tip. The Stanton number, however exhibits a more three-dimensional distribution. This is consistent with the findings of Tallman et al. (Ref. 8).

Unsteady Results

Figure 10 shows filled-in-contours of shock function at five different moments in time. Here, t, is not physical time but indicates time progression in steps. Starting at $t = 0$, the figure shows shock functions at 15, 25, 35, and 45 time steps after $t = 0$. The three sections shown in this figure are at (a) 15 percent span, (b) 50 percent span and (c) 90 percent span of the rotor blade. The shock function shows regions of large pressure gradients in the direction of velocity. So, regions colored in red are shocks while regions colored in blue are expansions. In Figures 10 and 11 some of these shocks and expansions have been marked with red and blue lines, respectively. The shock at the rotor leading edge, C1, moves from the crown on the suction side down towards the leading edge and weakens as it does so. Shock C1 can be seen reforming at $t = 25$. This phenomenon has been reported on by several authors including Denos et al. (Ref. 19) and Giles (Ref. 20). Close to the tip region, the shock begins to weaken and does not travel as much from the crown towards the leading edge. The rotor trailing edge shock at 90 percent span interacts with the shock from the upstream vane and dissipates before making contact with the suction side of the rotor. This interaction is indicated by shock structure C3 in Figure 10. At the leading edge, the passing of the upstream vanes causes a series of expansions shocks. Figure 11 shows filled-in-contours of shock function from the steady simulation at the same location. The steady solution shows that the shock, C1, is close to the crown of the rotor blade. The rotor trailing edge shock, C3, is well defined in both the steady and unsteady simulations and appears to be a steady phenomenon. The leading edge shock weakens in strength from the hub to the tip, at which point it vanishes.

Figure 12 shows Stanton number on the rotor surface at several instances in time. It appears that at the hub and tip, heat transfer is largely steady. The incoming thermal wake can be seen periodically washing over the suction side towards the leading edge causing lower heat transfer values at the leading edge compared to the steady solution. The steady analogue in Figure 6 shows a much higher heat transfer at the leading edge and lower heat transfer on the tip, near the leading edge. At the hub the heat transfer is much higher due to the interaction of the hub boundary layer with the flow, also known as the horseshoe vortex (Ref. 8). This region seems to be unaffected by unsteady effects.

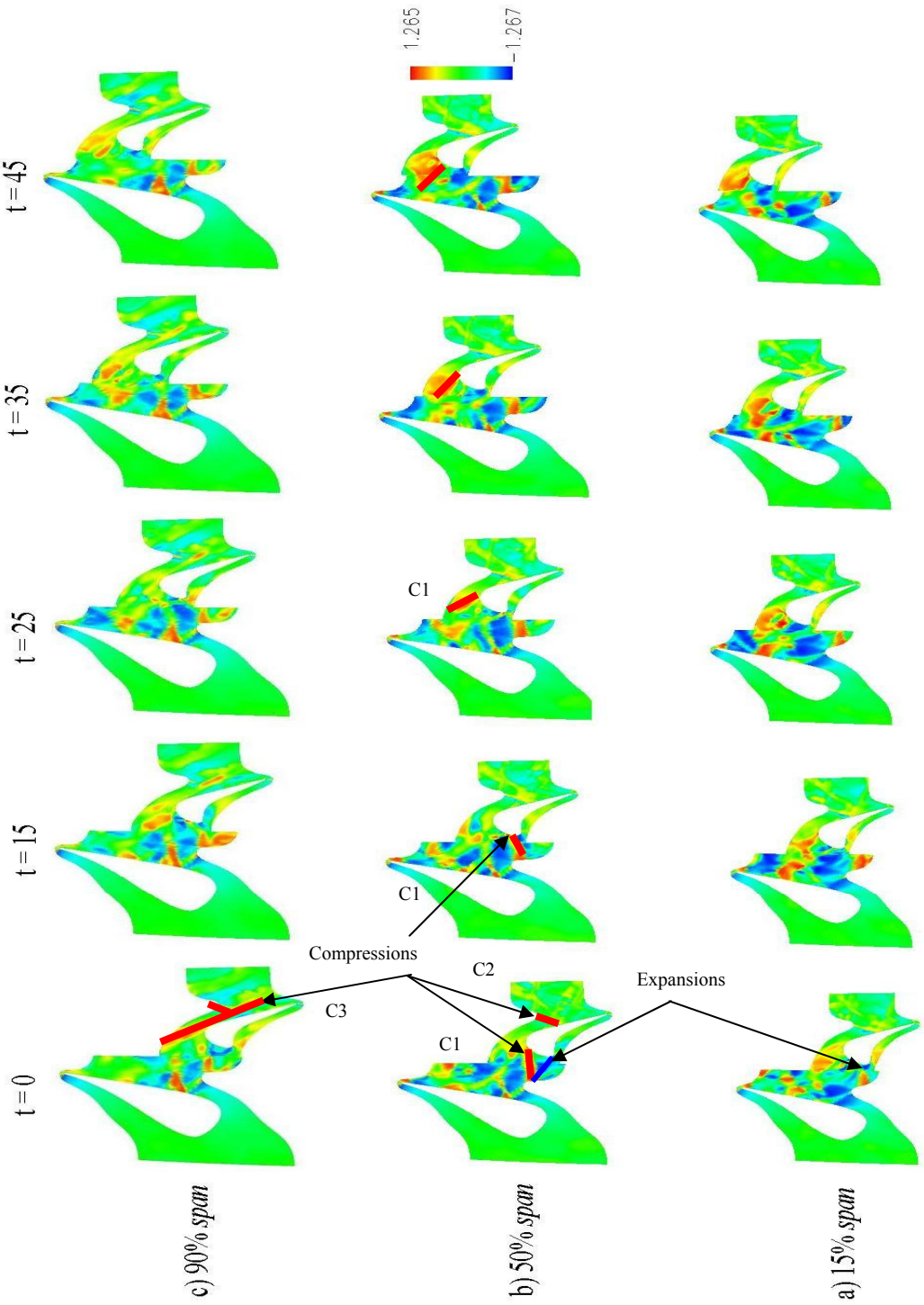

Figure 10.—Unsteady shock function at various span locations and at several instances in time.

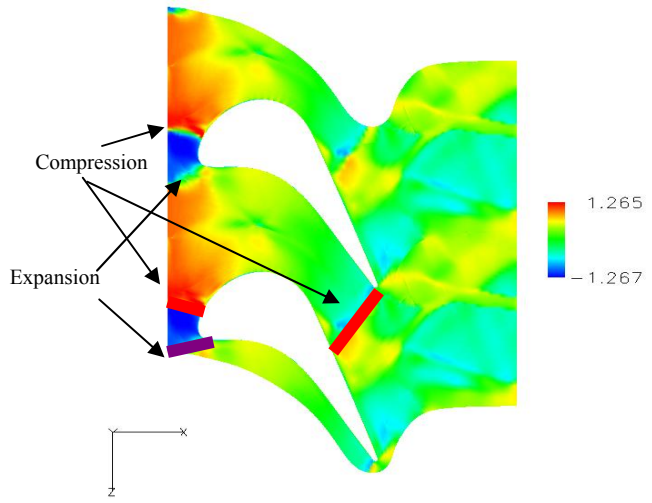

Figure 11.—Steady shock function at mid-span of rotor.

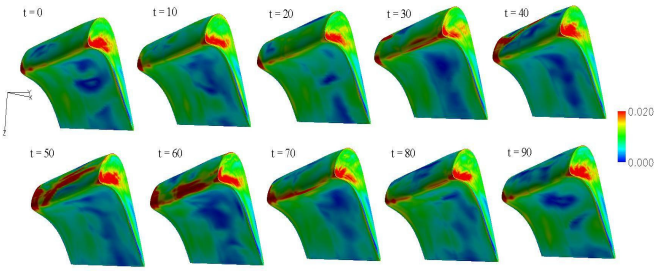

Figure 12.—Stanton number at various instances in time on the rotor blade.

HUB and Casing Heat Transfer and Pressure Analysis

Figures 13 and 14 show the heat transfer on the rotor hub and casing, respectively. On the hub, heat transfer is higher near the leading edge on the suction side while it is lower on the pressure side. This thermal segregation has been discussed earlier in this paper. On the casing, due to the clearance flow the heat transfer is seen to be lower than on the hub except in the region adjacent to the pressure side of the blade. This is probably because the hot air from the pressure side is being sucked towards the suction side and heats up the casing as it travels through the tip gap. These differences on the hub and the casing are easier to see in Figures 15 and 16, respectively that show the percent difference between the steady and time-averaged Stanton numbers. Percent difference was computed as,

$$\Delta_{St} = \frac{St_{\text{steady}} - St_{\text{time-averaged}}}{St_{\text{time-averaged}}} \times 100 \qquad (2)$$

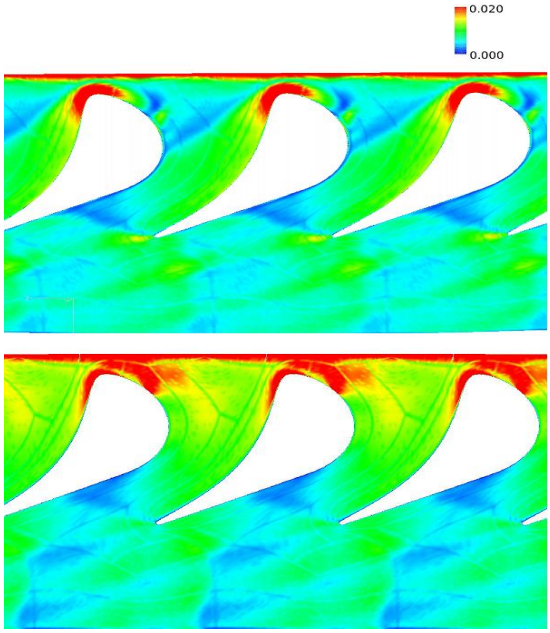

Figure 13.—Stanton number on rotor hub for steady (top) and time-average (bottom) of unsteady cases.

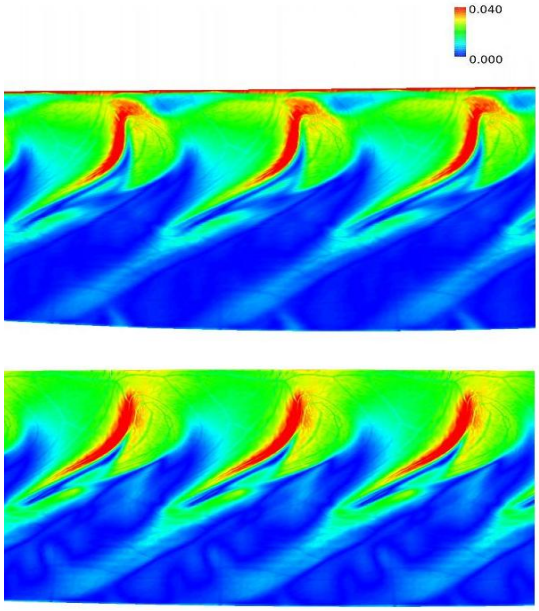

Figure 14.—Stanton number on rotor casing for steady (top) and time-average (bottom) of unsteady cases.

Figures 16 and 18 show an outline of the underlying grid to reveal the location of the rotor blade tip. On the hub, near the leading edge, there is almost a 100 percent difference between the steady and time-averaged cases. This can be attributed to the effect of the wake that interacts with the hub boundary layer. As seen in Figure 7, the hot gas travels radially outwards from the hub and causes the regions of the hub that are downstream of the leading edge to be cooler. At the casing the difference between the steady and time-averaged cases appears to be highly scattered based on Figure 16. This could be due to the complex interaction between the shocks C3 from

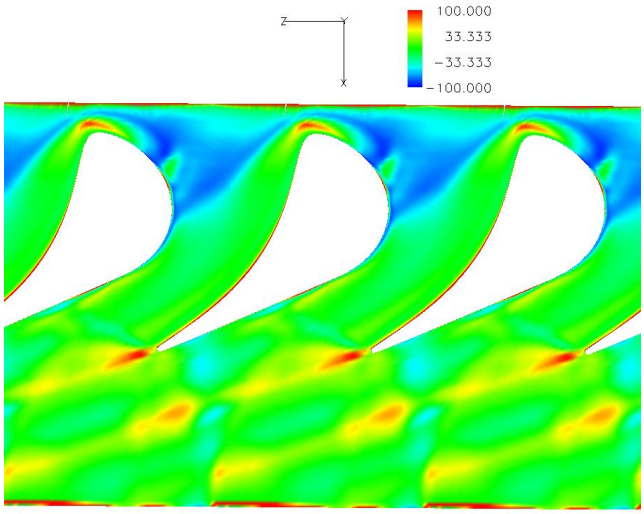

Figure 15.—Percent difference between steady and time-averaged Stanton number on rotor hub.

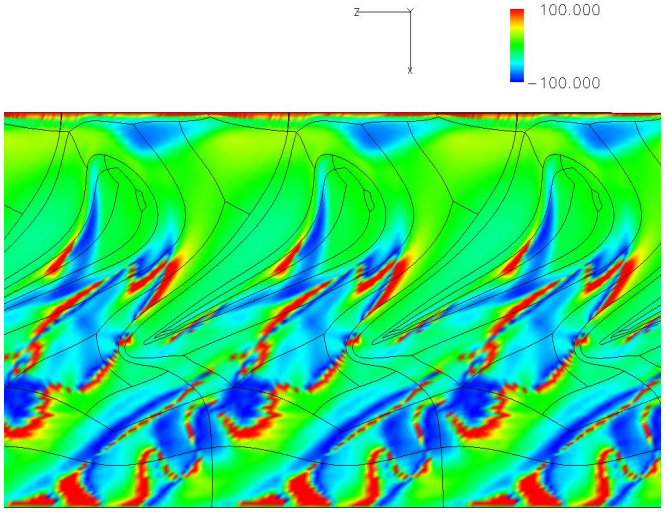

Figure 16.—Percent difference between steady and time-averaged Stanton number on rotor casing.

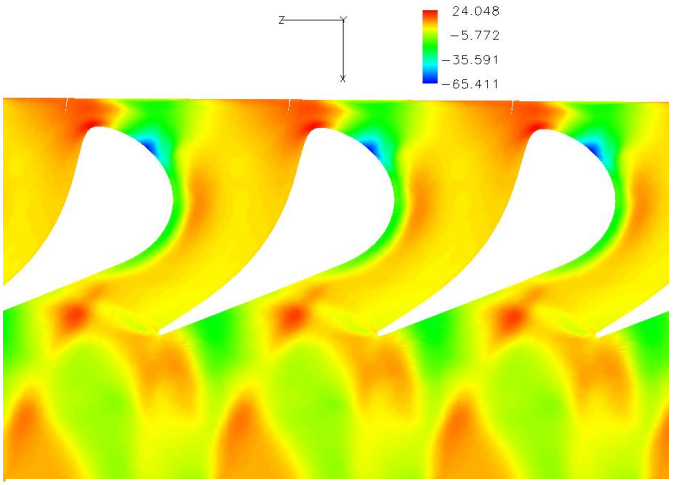

Figure 17.—Percent difference between steady and time-averaged pressure on rotor hub.

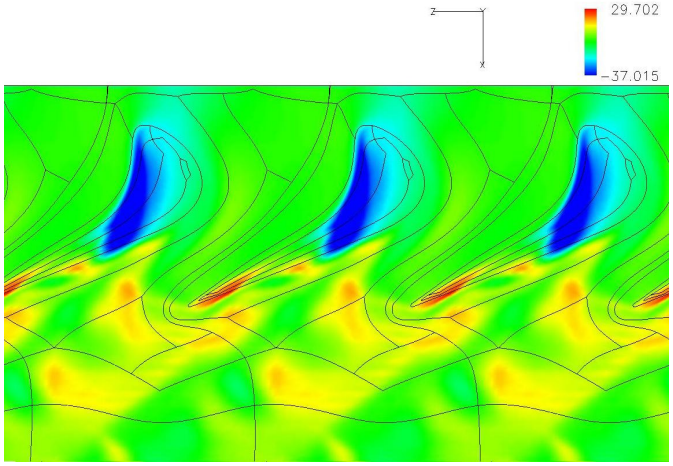

Figure 18.—Percent difference between steady and time-averaged pressure on rotor casing.

Figure 10, the rotor wake and the tip clearance flow. As mentioned in a previous section, the shock structure at the rotor trailing edge appears to be a steady phenomenon and so does the tip clearance flow. It stands to reason therefore that the differences seen in Figure 16 are due to the rotor wake and its interaction with the stator wake. Unlike at the hub, the stator wake has an influence downstream of the rotor as well. Figures 17 and 18 show percent differences between steady and time-averaged pressure results. Figure 17 shows the hub while Figure 18 shows the casing. The percent difference, Δ_p, is computed as,

$$\Delta_P = \frac{p_{\text{steady}} - p_{\text{time-averaged}}}{p_{\text{time-averaged}}} \times 100 \qquad (3)$$

On the hub, the pressure side shows up to 30 percent higher pressure values for the steady case than for the time-averaged case. On the suction side the blue island in Figure 17 corresponds to the region at which the stator shock meets the rotor blade. The pressure predicted by time-averaging the unsteady simulation is higher than the pressure predicted by the steady case. At the casing, the region in which the rotor and stator wakes interact show large differences in pressure between the steady and time-averaged cases as in the case of Stanton number.

Conclusions

A highly loaded high pressure turbine stage was simulated using the CFD code TURBO and unsteady results were compared to both experiment and steady results. It was found

that over most of the blade surface, the pressure calculated by the steady simulation is fairly accurate. However at the leading edge, the pressure field varies by large amounts between the steady and time-average of unsteady results. The heat transfer predicted by the steady simulation is lower than that predicted by the unsteady simulation except at the leading edge and near the trailing edge on the suction side. The thermal wake coming in to the rotor is thought to play a major role in explaining these differences. At the hub and casing significant differences in pattern and magnitude were observed between the steady and time-averaged CFD results. This is thought to be a result of thermal segregation as well as the interaction of the stator and rotor wakes near the casing. The simulations matched well with the data, but sufficient data is not available to match effects such as shocks and transition. It is recommended that for simulations involving film cooling at the leading edge and tip, the effect of unsteadiness be included especially if accurate heat transfer is of interest. While two-dimensional simulations can be accurate for prediction of pressure distribution close to mid-span, the pressure and heat transfer on the blade are highly three-dimensional. Therefore, if there is interest in studying heat transfer over the entire blade, a three-dimensional unsteady simulation should be performed.

References

1. Hodson, P., and Dawes, N., "On the Interpretation of Measured Profile Losses in Unsteady Wake-Turbine Blade Interaction Studies," ASME–96–GT–494, February 1996.
2. Denos, R., Arts, T., Paniagua, G., Michelassi, V., and Martelli, F., "Investigation of the Unsteady Rotor Aerodynamics in a Transoic Turbine Stage," ASME–2000–GT–435, January 2001.
3. Shang, T., and Epstein, A.H., "Analysis of Hot Streak Effects on Turbine Rotor Heat Load," ASME–96–GT–118, July 1997.
4. Ameri, A.A., Rigby, D.L., Steinthorsson, E., Heidmann, J., and Fabian, J.C., "Unsteady Analysis of Blade and Tip Heat Transfer as Influenced by the Upstream Momentum and Thermal Wakes," ASME–GT2008–51242, June 2007, Berlin, Germany.
5. Kerrebrock, J.L. and Mikolajczak, A.A., "Intra-Stator Transport of Rotor Wakes and Its Effect on Compressor Performance," Journal of Engineering for Power, vol. 92, no. 4, October 1970, pp. 359–368.
6. Bell, D.L., He, L., "Three-Dimensional Unsteady Flow for an Oscillating Turbine Blade and the Influence of Tip Leakage," ASME–98–GT–571, February 1998.
7. Urbassik, R.M., Wolff, J.M., and Polanka, M.D., "Unsteady Aerodynamics and Interactions Between a High Pressure Turbine Vane and Rotor," ASME–GT2004–53607, June 2004, Vienna, Austria.
8. Tallman, J.A., Haldeman, C.W., Dunn, M.G., Tolpadi, A.K., and Bergholz, R.F., "Heat Transfer Measurements and Predictions for a Modern, High-Pressure, Transonic Turbine, Including Endwalls," ASME–GT2006–90927, May 2006, Barcelona, Spain.
9. Luk, D.F., "Steady Heat Transfer Predictions for a Highly Loaded Single Stage Turbine With a Flat Tip," Master's Thesis, October 2008, The Ohio State University, Columbus, Ohio.
10. Holmes, D.G., Mitchell, B.E., and Lorence, C.B., "Three-Dimensional Linearized Navier-Stokes Calculations for Flutter and Forced Response," 8th International Symposium on Unsteady Aerodynamics and Aeroelsticity of Turbomachines, September 1997, Stockholm, Sweden.
11. Chen, J.P., and Whitfield, D.L., "Navier-Stokes Calculations for the Unsteady Flowfield of Turbomachinery," AIAA–93–0676, January 1993.
12. Chen, J.P., and Barter, J., "Comparison of Time-Accurate Calculations for the Unsteady Interaction in Turbomachinery Stage," AIAA–98–3292, July 1998.
13. Chen, J.P., and Briley, W.R., "A Parallel Flow Solver for Unsteady Multiple Blade Row Turbomachinery Simulations," ASME–2001–GT–0348. June 2001.
14. Zhu, J., Shi, T.H., "An NPARC Turbulence Module With Wall Functions," AIAA Paper no. 1996–0382.
15. Van Zante, D., Chen, J., Hathaway, M., and Chris, R., "The Influence of Compressor Blade Row Interaction Modeling on Performance Estimates From Tmie-Accurate, Multistage, Navier-Stokes Simulations," ASME–GT2005–68463, August 2006.
16. Gerolymos, G.A., Michon, G.J., and Neubauer, J., "Analysis and Application of Chorochronic Periodicity in Turbomachinery Rotor/Stator Interaction Computations," Journal of Propulsion and Power, vol. 18, no. 6, November-December, 2002.
17. Abhari, R.S., Guenette, R.G., Epstein, A.H., and Giles, M.B., "Comparison of Time-Resolved Turbine Rotor Blade Heat Transfer Measurements and Numerical Calculations," ASME–91–GT–268. March 4, 1991, Orlando, FL.
18. Herrick, G.P., "Facilitating Higher Fidelity Simulations of Axial Compressor Instability and Other Turbomachinery Flow Conditions," PhD Thesis, May 2008, Mississippi State University.
19. Green, B.R., Barter, J.W., Haldeman, C.W., and Dunn, M.G., "Averaged and Time-Dependent Aerodynamics of a High Pressure Turbine Blade Tip Cavity and Stationary Shroud: Comparison of Computational and Experimental Results," ASME–2004–GT–53443, October 2005.
20. Giles, M.B., "Stator/Rotor Interaction in a Transonic Turbine Stage," AIAA Paper no. 88–3093, 1988.

REPORT DOCUMENTATION PAGE	Form Approved OMB No. 0704-0188

1. REPORT DATE *(DD-MM-YYYY)*	2. REPORT TYPE	3. DATES COVERED *(From - To)*
01-02-2010	Technical Memorandum	

4. TITLE AND SUBTITLE
Three-Dimensional Unsteady Simulation of a Modern High Pressure Turbine Stage Using Phase Lag Periodicity: Analysis of Flow and Heat Transfer

5a. CONTRACT NUMBER

5b. GRANT NUMBER

5c. PROGRAM ELEMENT NUMBER

6. AUTHOR(S)
Shyam, Vikram; Ameri, Ali; Luk, Daniel, F.; Chen, Jen-Ping

5d. PROJECT NUMBER

5e. TASK NUMBER

5f. WORK UNIT NUMBER
WBS 561581.02.08.03.21.03

7. PERFORMING ORGANIZATION NAME(S) AND ADDRESS(ES)
National Aeronautics and Space Administration
John H. Glenn Research Center at Lewis Field
Cleveland, Ohio 44135-3191

8. PERFORMING ORGANIZATION REPORT NUMBER
E-17109

9. SPONSORING/MONITORING AGENCY NAME(S) AND ADDRESS(ES)
National Aeronautics and Space Administration
Washington, DC 20546-0001

10. SPONSORING/MONITOR'S ACRONYM(S)
NASA

11. SPONSORING/MONITORING REPORT NUMBER
NASA/TM-2010-216064

12. DISTRIBUTION/AVAILABILITY STATEMENT
Unclassified-Unlimited
Subject Categories: 02 and 34
Available electronically at http://gltrs.grc.nasa.gov
This publication is available from the NASA Center for AeroSpace Information, 443-757-5802

13. SUPPLEMENTARY NOTES

14. ABSTRACT
Unsteady three-dimensional RANS simulations have been performed on a highly loaded transonic turbine stage and results are compared to steady calculations as well as experiment. A low Reynolds number k-ε turbulence model is employed to provide closure for the RANS system. A phase-lag boundary condition is used in the periodic direction. This allows the unsteady simulation to be performed by using only one blade from each of the two rows. The objective of this paper is to study the effect of unsteadiness on rotor heat transfer and to glean any insight into unsteady flow physics. The role of the stator wake passing on the pressure distribution at the leading edge is also studied. The simulated heat transfer and pressure results agreed favorably with experiment. The time-averaged heat transfer predicted by the unsteady simulation is higher than the heat transfer predicted by the steady simulation everywhere except at the leading edge. The shock structure formed due to stator-rotor interaction was analyzed. Heat transfer and pressure at the hub and casing were also studied. Thermal segregation was observed that leads to the heat transfer patterns predicted by steady and unsteady simulations to be different.

15. SUBJECT TERMS
Rotors; Stators; Unsteady flow; Heat transfer

16. SECURITY CLASSIFICATION OF:			17. LIMITATION OF ABSTRACT	18. NUMBER OF PAGES	19a. NAME OF RESPONSIBLE PERSON
a. REPORT	b. ABSTRACT	c. THIS PAGE			STI Help Desk (email:help@sti.nasa.gov)
U	U	U	UU	17	19b. TELEPHONE NUMBER *(include area code)* 443-757-5802